Fiber-optic fluorescence imaging

Benjamin A Flusberg, Eric D Cocker, Wibool Piyawattanametha, Juergen C Jung, Eunice L M Cheung & Mark J Schnitzer

Optical fibers guide light between separate locations and enable new types of fluorescence imaging. Fiber-optic fluorescence imaging systems include portable handheld microscopes, flexible endoscopes well suited for imaging within hollow tissue cavities and microendoscopes that allow minimally invasive high-resolution imaging deep within tissue. A challenge in the creation of such devices is the design and integration of miniaturized optical and mechanical components. Until recently, fiber-based fluorescence imaging was mainly limited to epifluorescence and scanning confocal modalities. Two new classes of photonic crystal fiber facilitate ultrashort pulse delivery for fiber-optic two-photon fluorescence imaging. An upcoming generation of fluorescence imaging devices will be based on microfabricated device components.

Fiber-optic fluorescence imaging has become increasingly versatile over the last decade as fiber-based devices have declined in size but gained in functionality. Three classes of applications in live animal and human subjects provide the primary motivations for innovation in fiber-optic imaging. First, basic research on biological and disease processes would benefit enormously from instrumentation that permits cellular imaging under conditions in which conventional light microscopy cannot be used. Many cell types reside within hollow tissue tracts or deep within solid organs that are inaccessible to optical imaging without devices that can reach such locations in a minimally invasive manner. Flexible fiber-optic devices also allow handheld imaging and imaging in freely moving animals[1]. Second, fiber devices might be implanted within live subjects for long-term imaging studies. This capability will not only benefit research on the cellular effects of aging, development or experience, but also will lead to new *in vivo* assays for testing of drugs and therapeutics. By allowing examination of cells concurrently with observation of disease symptoms and animal behavior, fiber-optic imaging will permit studies correlating cellular properties and disease outcome in individual subjects over time and could reduce the numbers of animals needed. A third set of applications concerns development of minimally invasive clinical diagnostics and surgical procedures[2]. Although much work remains, fiber-optic instrumentation has already broadened the applicability of *in vivo* fluorescence imaging.

The seeds for development of fiber optic *in vivo* imaging were planted by early uses of fiber-optics and fluorescence for chemical sensing and spectroscopy, including classic work on detection of intracellular redox states[3–5]. Use of fiber optics for remote sensing and spectroscopy remains strong today[6], and has expanded to include bioluminescence detection[7]. The recent proliferation of fluorescent probes has widened the set of potential uses for fiber-based fluorescence imaging devices, which may be classified by size into the three broad categories of microscopy, endoscopy and microendoscopy.

The simplest application of fiber-optics in microscopy is remote delivery of light[8–16], which allows the excitation light source or photodetectors to reside apart from a conventional microscope. Optical fiber also enables miniaturized or compact forms of microscopy for portable usage[1,17,18]. Flexible fiber-optic endoscopy involves optical probes that are usually a few millimeters in diameter and well suited to imaging either superficial tissues such as skin or hollow tissue cavities such as the cervix or digestive tract[19–34]. Fluorescence microendoscopy (FME) involves optical probes that are typically 0.25–1 mm in diameter for minimally invasive insertion into solid tissue. Such probes can either be mainly rigid and one to several centimeters in length, for use akin to a

James H. Clark Center for Biomedical Engineering and Sciences, Stanford University, 318 Campus Drive, Stanford, California 94305, USA. Correspondence should be addressed to M.J.S (mschnitz@stanford.edu)

PUBLISHED ONLINE 18 NOVEMBER 2005; DOI:10.1038/NMETH820

needle biopsy[35–37], or mated to flexible fiber optics[38–43]. Both types of FME have allowed cellular imaging deep within solid tissues of live mammalian subjects[2,35,37,38,42,44].

All three categories of fiber-based imaging, microscopy, endoscopy and microendoscopy, can involve the fluorescence modalities reviewed elsewhere in this issue, including one-photon epifluorescence, scanning confocal fluorescence and two-photon excited fluorescence. Many strengths and limitations of the conventional tabletop systems also characterize the corresponding fiber-optic forms (Table 1). We focus here on components and embodiments that are particular to fiber-based imaging to help readers choose and construct imaging devices best suited to their needs.

COMPONENTS

Several features of fiber-optic imaging systems are nearly universal. Optical fiber delivers illumination, and one or more lenses focus this light at the specimen plane and collect fluorescence emissions. In many cases a focusing mechanism allows adjustment of the imaging plane. For confocal and two-photon modalities, a scanning mechanism moves one or more focal spots across the field of view.

Optical fiber

Optical fiber commonly ranges from ~80 μm up to several millimeters in diameter and can perform many jobs, including light delivery and collection, as well as image transmission. How are these functions accomplished? In conventional fibers, known as step-index fibers, there are two zones with distinct indices of refraction, an outer cladding and an inner core, which enable light transmission down the fiber axis by total internal reflection[45]. A subclass of step-index fibers called single-mode fiber (SMF) guides only a single spatial mode of light (Box 1). SMF, which is widely available commercially, is well suited for illumination delivery in the scanning imaging modalities because the single spatial mode can be focused to a near diffraction-limited spot in the specimen plane, allowing high-resolution imaging. The same SMF core that delivers light can also act as a pinhole detector, rejecting out-of-focal plane fluorescence emissions[8–11,13–15,43,46,47].

Fibers that guide more than one spatial mode are called multimode fibers (Box 1). Step-index multimode fibers are better suited for fluorescence collection than SMF, because not only do they possess larger core diameters, commonly ~50 μm up to a few millimeters, but they also usually have greater numerical aperture (NA) values. All-polymer multimode fibers tend to be more flexible than their silica counterparts and are available with NA values up to ~0.5.

In a particular class of multimode fiber known as gradient refractive index (GRIN) fiber, the refractive index in the core declines approximately quadratically with radius from the central axis. Unlike in step-index multimode fibers, in GRIN fibers the different electro-

Table 1 | A comparison of fiber-optic fluorescence imaging modalities

Embodiments	Advantages	Limitations
EPIFLUORESCENCE	Ease of use, full-frame acquisition for high-speed imaging. Low-cost incoherent light source. Viewing through eyepieces or by camera.	Lack of optical sectioning, not robust to light scattering.
One-photon FME[35,79]	Proximal focusing with external objective lens.	GRIN endoscope probes are short and rigid.
Fiber-bundle epifluorescence[59]	Mechanical flexibility. Ease of handheld use.	Pixilation of image reduces resolution. Distal focusing mechanism hinders miniaturization.
CONFOCAL FLUORESCENCE	Optical sectioning. Laser source much less costly than for two-photon imaging.	Not robust to light scattering, penetration depths of ~50 μm in tissue. Distal focusing mechanism hinders miniaturization.
Single-fiber confocal[22,24,26–29,67–69]	Mechanical flexibility. Single fiber for both excitation delivery and emission collection.	Distal scanning mechanism hinders miniaturization.
Dual-axis fiber confocal[81–83]	Mechanical flexibility. High axial resolution. Long working distance optics allow post-objective scanning for large fields of view and reduced aberrations.	Distal scanning mechanism hinders miniaturization. Reduced fluorescence collection efficiency because of the low-NA collection aperture.
Fiber-bundle confocal[19,23,25,30,31,40,42]	Mechanical flexibility. Ease of handheld use. Proximal scanning mechanism facilitates miniaturization. Line scanning can enable fast frame rate imaging.	Pixilation of image reduces resolution.
TWO-PHOTON FLUORESCENCE	Optical sectioning. Reduced photobleaching and photodamage. Robustness to scattering. Penetration depths in tissue up to ~300 μm.	Cost of ultrashort-pulsed laser.
Two-photon FME[35–37]	Proximal focusing with external objective lens. Proximal scanning. Minimal pulse dispersion and SPM.	GRIN endoscope probes are short and rigid.
Single-fiber two-photon[1,38,43]	Mechanical flexibility. No pulse distortion in PBF for zero-dispersion wavelength. Reduced SPM in LMA-PCF.	Distal scanning and focusing mechanisms hinder miniaturization. Dispersion compensation may be needed.
Fiber-bundle two-photon[39]	Mechanical flexibility. Proximal scanning. Ease of handheld use.	Pixilation of image reduces resolution. Distal focusing mechanism hinders miniaturization. Dispersion compensation needed. SPM at higher pulse energies.
Multi-focal two-photon[17,18]	Mechanical flexibility. Lens array enables high-speed multi-focal imaging. No pulse distortion in PBF for zero-dispersion wavelength. Reduced SPM in LMA-PCF.	Currently too large for endoscopy. Distal scanning and focusing mechanisms hinder miniaturization. Multiple foci decrease robustness to light scattering.
Double-clad two-photon[57,58]	Mechanical flexibility. Fluorescence collection and excitation delivery achieved in one fiber. Reduced SPM in LMA-PCF.	Distal scanning and focusing mechanisms hinder miniaturization. Dispersion compensation needed.

Abbreviations: self-phase modulation (SPM); photonic bandgap fiber (PBF); large mode area photonic crystal fiber (LMA-PCF).

magnetic spatial modes comprising an image propagate at nearly the same velocity. This means that GRIN fibers can serve as lenses when cut to specific lengths (see Objective optics below), enabling remote adjustment of the focal plane in the specimen using optics placed on the opposite side of the fiber[48]. The number of guided spatial modes in a GRIN medium limits the optical resolution of the transmitted image. This situation contrasts with how a fiber bundle transmits a pixilated image composed of an array of light intensities, in which case an optical focal mechanism must reside on the fiber side proximal to the specimen (see Fiber bundles below).

Important issues arise in two-photon fiber-optic imaging concerning the remote delivery of the ultrashort optical pulses (~80–250 fs in duration) typically used for two-photon excitation (Box 1). Particularly for *in vivo* studies, it is common to use pulses of nanojoule energies for two-photon imaging up to hundreds of micrometers deep within tissue. Such brief pulses are so intense that a light-matter interaction in the glass fiber core can distort both the pulse shape and spectrum through a nonlinear process known as self-phase modulation (SPM). This effect makes it challenging to excite two-photon fluorescence efficiently using SMF[49–51]. A newly developed class of

BOX 1 OPTICAL FIBER AND ULTRASHORT PULSE DELIVERY

OPTICAL FIBER

Single mode fibers

In step-index optical fibers, the fiber core has a refractive index (n_1) that is typically 1–2% higher than that of the cladding (n_2), leading to a numerical aperture NA = $(n_1^2 - n_2^2)^{1/2}$ equal to the sine of the half-angle of the cone of light emitted from the fiber. The solutions to Maxwell's equations with boundary conditions appropriate for electromagnetic wave propagation down a cylindrically symmetric fiber dictate that a fiber with a core radius a guides only a single spatial mode of light if the wavelength λ in vacuum satisfies the inequality $V < 2.405$, where the quantity $V = (2\pi a\ \mathrm{NA})/\lambda$ is known as the 'normalized wave number'[45]. Such fibers are single-mode and have typical core diameters of ~3–7 μm for visible light.

Multimode fibers

If $V > 2.405$ the fiber can guide more than one spatial mode. The number of transmitted spatial modes increases approximately quadratically as a function of V, and so-called multimode fibers operate in the limit in which the number of guided modes is large, usually a hundred or more. Multimode fibers have core diameters of ~50 μm up to several millimeters.

GRIN fibers and lenses

In cylindrically symmetric GRIN lens and fibers the refractive index commonly varies as $n(r) = n_0(1 - g^2r^2/2)$, where r is the radius from the fiber axis, n_0 is the refractive index on axis and g is a constant parameter. In a ray description, paraxial light rays follow an approximately sinusoidal path with a period of length $P = 2\pi/g$ as they propagate down the cylindrical axis of a GRIN medium[45]. Thus, two primary determinants of the properties of a GRIN lens are the lens length and refractive index profile.

ULTRASHORT PULSE DELIVERY IN OPTICAL FIBER

Ultrashort pulses of ~80–250 fs duration and nanojoule energies are commonly used to induce two photon–excited fluorescence *in vivo*. When such pulses propagate through an optical fiber, both group velocity dispersion and self-phase modulation can distort the pulse's temporal profile and impact the efficiency of two-photon excitation, which varies inversely with pulse duration.

Group velocity dispersion

Chromatic or group velocity dispersion (GVD) occurs when different colors of light travel through optical fiber or other optical components at distinct speeds, thereby incurring differential propagation delays. In optical fiber there are two sources of GVD, known as material and waveguide dispersion. Material dispersion results from the different speeds at which each spectral component travels through silica glass[45]. Waveguide dispersion arises because a different proportion of the pulse energy at each wavelength propagates through the fiber cladding. These two components cancel at the so-called zero-GVD wavelength. Configurations of diffraction gratings[55] or prisms[56] can compensate for GVD by negatively 'pre-chirping' optical pulses—that is, giving wavelengths that travel more slowly through optical fiber a head start, so that all spectral components exit the fiber simultaneously. This counteracts GVD, which by itself yields pulses that are positively chirped and temporally broadened.

Self-phase modulation

Intense laser pulses interact with the silica core in SMF and transiently raise the local refractive index. This index rise induces a phase shift and a corresponding spectral distortion in the pulse through self-phase modulation (SPM), which occurs in a nonlinear manner that depends on the pulse's temporal profile of wavelength and intensity[45]. Because of this nonlinear dependence it is difficult to compensate for SPM, which leads to spectral narrowing and temporal broadening of negatively pre-chirped pulses propagating in SMF, for wavelengths shorter than the zero-GVD wavelength of 1.3 μm[49–51]. Hollow-core PBF (**Fig. 1a**) and LMA-PCF (**Fig. 1b**) ameliorate the problems associated with SPM and can deliver ultrashort pulses with little distortion.

Exploiting nonlinear pulse distortion

It is possible to harness nonlinear effects in optical fiber to alter the pulse spectrum for particular two-photon imaging applications[12,90,91]. Small core (~1- to 3-μm diameter) or 'highly nonlinear' photonic crystal fibers can enhance SPM-induced spectral broadening of positively chirped ultrashort pulses below the zero-GVD wavelength (**Fig. 1d**). Subsequent temporal recompression of the pulses can increase the two-photon fluorescence excitation efficiency by up to almost an order of magnitude[91]. The spectral broadening created by SPM can also enable the excitation of dyes, such as fura-2, whose two-photon absorption spectra are below the wavelength range of most common ultrashort laser sources[90].

Measurements of pulse width

A simple means of characterizing the temporal width of ultrashort pulses is to use an autocorrelator, which splits the beam between two paths and then recombines these on a nonlinear detector. Because the two pulses from the separate paths must arrive almost coincidentally at the nonlinear detector to register the maximum amplitude signal, pulse duration can be inferred from how the detector signal changes as the relative path length between the two paths varies. Other pulse diagnostics, such as frequency-resolved optical gating, can provide information about both the intensity and wavelength temporal profiles.

optical fiber known as photonic crystal or microstructured fiber can be used either to circumvent or harness SPM.

Photonic crystal fiber is named after the periodic arrays of air holes and silica glass these fibers exhibit within their internal structure (Fig. 1). Many forms of silica-core microstructured fiber guide light by a modified form of total internal reflection, in which the effective refractive index of the air-silica array in the cladding is less than that of the core. Photonic bandgap fiber (PBF) is a form of microstructured fiber that does not rely on total internal reflection for guiding light (Fig. 1a).

PBF uses diffractive effects that arise from interactions between light and internal air-silica arrays with structure at the same length scale as the wavelength. A carefully designed air-silica lattice creates a photonic bandgap analogous to an electronic bandgap in crystalline solids, which prevents light within a certain wavelength range from propagating in the cladding. An air core within such a PBF can act as a lattice defect, localizing light to the core, much as crystalline solid defects create localized electronic states. Wavelengths within the bandgap are thus contained and transmitted within the core, with the lowest-order mode typically having a Gaussian-like spatial profile[52]. PBF has transformed the possibilities for fiber-based two-photon excited fluorescence and other nonlinear optical imaging modalities, because even high-energy pulses do not undergo SPM in an air core. Moreover, within the transmission window of PBF, which is called the bandgap and usually covers a spectral range of several tens to over a hundred nanometers, there is usually a wavelength at which group velocity (chromatic) dispersion vanishes (Box 1). Pulses centered at this wavelength scarcely suffer any broadening, making PBF an excellent choice for pulse delivery[16,17,38,53,54]. For other transmitted wavelengths only tens of nanometers away, however, dispersive pulse broadening can be more severe than in conventional SMF. Application of basic methods for dispersion compensation[55] can alleviate much of such broadening (Box 1), but for fiber lengths greater than a few meters additional compensation for 'higher-order' dispersion might also be required[38,56].

A good alternative means for delivery of ultrashort pulses involves a class of microstructured fiber known as large mode area photonic crystal fiber (LMA-PCF; Fig. 1b). These low-NA fibers not only have a large core of up to ~35 µm in diameter, in which pulse intensity is much reduced compared to the ~5–6 µm core of SMF, but also are 'endlessly single mode' in that only one spatial mode propagates regardless of wavelength within the silica transparency window. The reduced intensity diminishes, but does not eliminate SPM. Group velocity dispersion can be compensated using basic approaches because higher order dispersion appears to be much less important than in current forms of PBF. An especially interesting LMA-PCF for two-photon imaging is a 'double-clad' fiber that is essentially two fibers in one and can accomplish both excitation pulse delivery and fluorescence emission collection[57,58]. An inner LMA core delivers ultrashort pulses, and together with an inner cladding also serves as the core for a surrounding multimode fluorescence collection fiber (Fig. 1c). An outer multimode fiber cladding is composed almost entirely of air, leading to a high NA for visible light collection up to ~0.6. Use of such double-clad fiber for two-photon microscopy has been demonstrated[57,58]. All types of photonic crystal fiber discussed here are commercially available.

Fiber bundles

Fiber-optic bundles consist of up to ~100,000 individual step-index fibers in a closely packed arrangement, hundreds of micrometers to a few millimeters in total diameter. Image-guiding bundles maintain the relative arrangements of the individual fibers throughout the length of the bundle, allowing transmission of an intensity image in pixilated form. Such bundles are commercially available and are commonly used for both epifluorescence[59] and scanning confocal or two-photon imaging[19,23,25,30,31,39,40,42,60–62]. However, unlike in lenses or GRIN fibers, only intensity information is transmitted. This limitation can hinder miniaturization if one desires a built-in focusing mechanism that does not require moving the entire imaging head, because such a mechanism has to be engineered within the optics proximal to the specimen[25,30,31]. Many devices based on fiber bundles lack such focal capability, sacrificing functionality for size reduction[39,40,42]. On the other hand, use of a fiber bundle facilitates miniaturization of laser-scanning modalities by allowing scanning mechanisms to reside on the side of the bundle distal to the specimen for sequential illumination of the individual fibers (Fig. 2a–c).

The main disadvantage of fiber bundles is that pixilation reduces the lateral optical resolution in the specimen plane to about twice the average core-to-core distance between fibers divided by the optical magnification of the imaging lenses. Furthermore, the thin layer of cladding between adjacent fiber cores leads to optical cross talk in which light from neighboring image pixels can leak into one another, reducing contrast. In scanning confocal imaging this problem may be reduced by use of a nonordered bundle, in which the relative fiber positions are randomized and not maintained throughout the bundle. This approach requires having to reconstruct the sample image based on knowledge of the scrambled fiber arrangement, but helps to reduce cross talk. Nonordered bundles are especially useful for laser line-scanning forms of fast confocal imaging, in which adjacent fibers at one side of the bundle are illuminated concurrently but the resulting fluorescence originates from physically separate locations in the sample[62]. In all fiber-bundle applications, calibration of the intrinsic

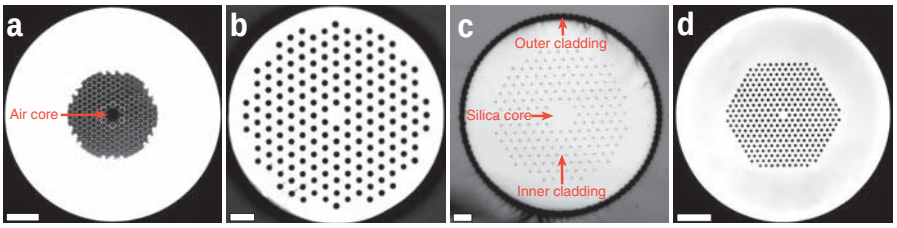

Figure 1 | Photographs of photonic crystal fibers. (**a**) Hollow-core PBF. Wavelengths within the transmission band are localized to the air core, virtually eliminating SPM. (**b**) Large-mode area photonic crystal fiber (LMA-PCF). Light guidance in the silica core is 'endlessly single mode' and the large mode area reduces SPM. (**c**) Double-clad photonic crystal fiber. A silica LMA core and a surrounding air-silica inner cladding comprise an inner lower-NA fiber that can guide ultrashort pulses with reduced SPM. An outer cladding composed nearly exclusively of air creates a higher-NA fiber that can collect fluorescence efficiently. Acrylate structural support surrounds the outer cladding and is not fully shown. (**d**) Highly nonlinear photonic crystal fiber. The small silica core can be used to harness SPM for broadening the spectrum of ultrashort excitation pulses. Scale bars, 20 µm. Photographs kindly provided by R. Kristiansen (Crystal Fibre A/S).

autofluorescence, precise position and optical throughput for each fiber in the bundle can facilitate postacquisition image processing and substantially improve image quality[42].

Objective optics

For applications without severe size constraints, a conventional microscope objective lens nearly always provides superior optical resolution and fluorescence detection efficiency. When miniaturization is required, custom high-NA (0.46–1.0)[19,23,30,31] objective lenses can be designed with outer diameters as small as 3–7 mm. Use of injection-molded plastic lenses to construct a custom objective is a particularly lightweight and economical approach[23].

The creation of minimally invasive microendoscope probes has benefited greatly from recent advances in the fabrication of GRIN microoptics. GRIN microlenses ranging from 350–1,000 μm in diameter have been used for one-photon, confocal and two-photon FME[35–40,43]. As in GRIN fiber, cylindrical GRIN lenses exhibit a refractive index that declines approximately quadratically with radius (Box 1). Compound GRIN microendoscope probes usually measure one or more centimeters in length and combine two or more GRIN lenses with different characteristics[35–37]. These are typically a 0.4–0.6 NA objective lens that enables micrometer-scale resolution and a longer relay lens that projects a real image of the specimen plane and supplies sufficient length for reaching deep tissue[35–37]. Optical aberrations in current GRIN lenses limit the resolving power to approximately twice the diffraction limit[35–38]. A detailed description of GRIN endoscope probes is available in ref. 35, and custom GRIN lenses are available from multiple vendors.

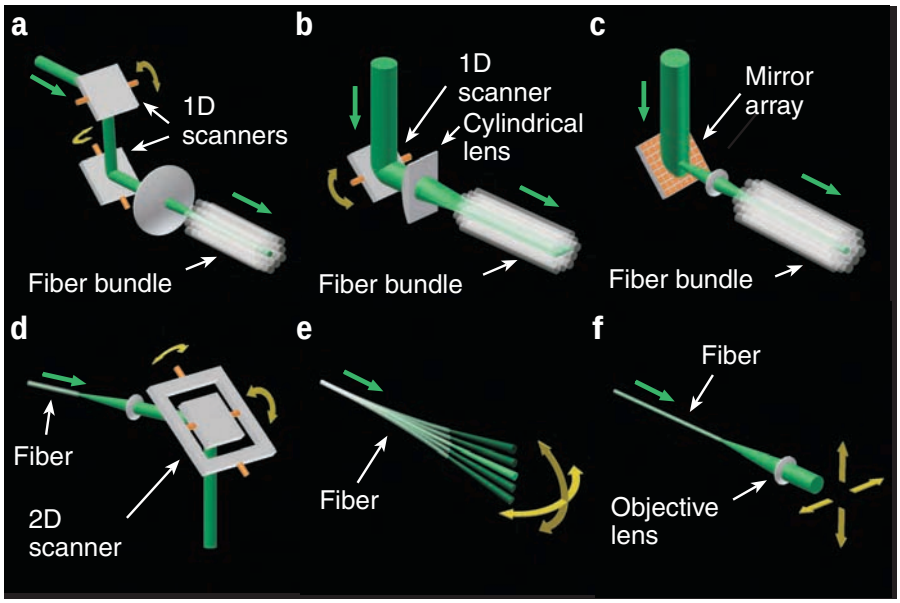

Figure 2 | Scanning mechanisms. (**a**) Proximal scanning. Cascaded galvanometer-mounted mirrors scan the excitation beam across the proximal end of a fiber bundle. (**b**) Proximal line-scanning. A cylindrical lens focuses the illumination to a line that is scanned across the face of a fiber bundle in one dimension. (**c**) Proximal scanning with a spatial light modulator, which can illuminate pixels sequentially without sweeping the beam. (**d**) Distal 2D mirror scanning. A piezoelectric driven tip-tilt mirror or a miniaturized MEMS mirror pivots in two angular dimensions. (**e**) Distal fiber tip scanning. The tip of the excitation delivery fiber is vibrated at resonance by an actuator (not shown). (**f**) Distal fiber-objective scanning. Both the fiber and the objective lens are mounted together on a cantilever (not shown) that is vibrated at resonance by an actuator.

Scanning mechanisms

It is common to speak of scanning mechanisms as being either proximal or distal to the light source. Proximal scanners are located in the illumination pathway upstream of the fiber and are used with a fiber bundle. Distal scanners are located on the fiber side distal to the light source and usually scan illumination from a single fiber over the specimen. Proximal scanning offers the benefit of separating bulky scanners from a miniaturized imaging head and typically involves a pair of galvanometer-mounted scanning mirrors (Fig. 2a)[19,23,25,30,31,39,40,42,61,62]. These can provide high image-acquisition rates (up to ~1 kHz per image line), particularly in a fast line-scanning approach that can allow video-rate imaging (Fig. 2b), and optical deflection angles up to ~40°. However, because the galvanometer approach involves sweeping the illumination across the bundle, light enters the cladding between adjacent cores during much of the scanning cycle, potentially diminishing image contrast.

Use of a spatial light modulator such as a pixilated micromirror array to illuminate each fiber sequentially, without sweeping the beam, can reduce errant excitation light (Fig. 2c)[60]. Nonetheless, much of the excitation power is lost, because although the entire modulator is illuminated with light, only a fraction of the pixels will be activated at any given moment during a scan. This loss may not pose much problem for imaging at superficial tissue depths. Both one-dimensional (1D) and two-dimensional (2D) spatial light modulators are available commercially.

The use of a single fiber for illumination delivery necessitates a distal scanning mechanism. Portable microscopy can rely on a piezoelectric-driven, 2D tip-tilt mirror (Fig. 2d), which has a lower bandwidth (~200 Hz) but a smaller footprint than cascaded galvanometers[17,18,63]. However, endoscopy and microendoscopy require more compact scanning mechanisms. One approach relies on either a piezoelectric[1,38,64] or an electromagnetically excited[65,66] actuator to drive mechanical resonance vibrations of the fiber tip (Fig. 2e). Although fiber tip scanning allows stationary imaging optics to be inserted into solid tissue[38], it can also introduce off-axis aberrations that might limit the achievable resolution. To preclude such aberrations, one can attach both the fiber and the imaging lens to a resonant cantilever and scan them together using electrostatic forces[67] or piezoelectric actuators[20,24] (Fig. 2f). Although this method needs an actuator that delivers more force, the required angular scanning range is reduced because the scanned focal spot is not further demagnified. A disadvantage of resonant scanning is that it is usually not possible to offset the center of the image field from the main optical axis without addition of another deflector.

In recent years, microfabricated microelectromechanical systems (MEMS) torsion scanning mirrors ~0.5–2 mm in diameter have emerged as versatile miniaturized scanning mechanisms (Figs. 2d and 3)[68–70]. MEMS scanners are created through sequential material etch-

ing and deposition processes analogous to those used for integrated circuit fabrication; 2D scanning involves cascaded 1D scanners or a single 2D scanner. The latter simplifies the optical design and reduces overall size. MEMS scanners that rely on electrostatic actuation are the most commonly used owing to the small size, low power consumption and high force that can be achieved. Among the electrostatic actuators, vertical comb actuators[71–73] offer greater force and angular range than parallel plate actuators[68,69]. These interdigitated silicon comb actuators provide electrostatic torque to rotate the mirror in one direction, and torsional springs supply a restoring torque (Fig. 3). Operating such scanners in DC mode permits static offsets of the field of view and mechanical angular rotations of up to ~6° (ref. 71). Alternatively, because ~1-mm-diameter MEMS mirrors have mechanical resonance frequencies in the kHz range, resonance scanning can enable video-rate imaging with large angular mirror rotations (>30°)[72], albeit at the expense of not being able to make lateral offsets in the field of view. A disadvantage of MEMS scanners is that although they are ideal for miniaturization, their fabrication requires much expertise. However, MEMS scanning mirrors are becoming commercially available.

Focusing mechanisms

Many applications benefit from having a built-in mechanism for altering the image focus without having to move the entire imaging probe. As with scanners, such mechanisms are positioned either proximal or distal to the light source relative to the fiber. Distal focusing mechanisms tend to hinder miniaturization because they are integrated with the objective optics, whereas proximal mechanisms are of conventional size and do not enter the specimen. For instance, it can be helpful to leave a GRIN microendoscope probe stationary within tissue while adjusting the image plane by moving the external microscope objective lens that also delivers illumination into the probe[35,37,74]. Because of optical demagnification between image and object planes, a focal shift of ~100 micrometers in the tissue often requires movement of focusing optics over millimeter-sized distances, beyond the range of small piezoelectric actuators. For flexible modalities that require distal focusing, one can use a hydraulic or pneumatic system to move the end of a fiber with respect to the objective optics when a fluid is injected into or withdrawn from a reservoir[25,30,31]. Another lightweight approach relies on a miniature motor to alter the distance between the fiber and the imaging optics[38]. In the future, millimeter-sized liquid lenses that alter their focus via electrowetting, will allow fast, remotely controlled distal focusing and beam steering for endoscopy and FME[75–77].

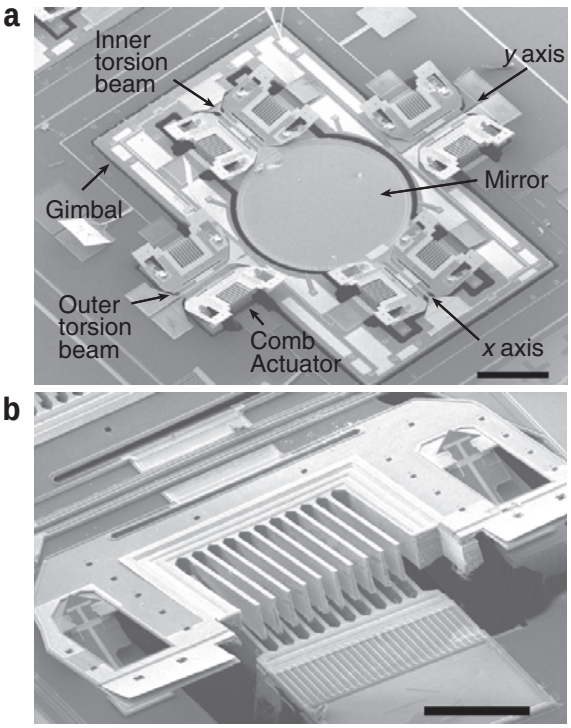

Design and integration

As imaging systems have become increasingly miniaturized, optical and mechanical designs have grown increasingly intricate. Zemax and Code V are optical ray-tracing software programs that are commonly used for optical design and tolerance analysis. Computer-aided design programs such as SolidWorks and AutoCad can generate 3D models and technical drawings of mechanical configurations. We have found such software invaluable for designing complex imaging systems.

EMBODIMENTS

Fiber-optic epifluorescence, scanning confocal and two-photon imaging each has distinct sets of strengths and limitations[78] (Table 1). The latter two forms offer 3D optical sectioning, important for many applications, but sectioning is not always needed or desired. For example, *in vivo* epifluorescence microendoscopy readily allows viewing, by eye or with video-rate recordings, of red blood cell flow, without the need for laser sources or fast scanners[35,44]. Further, lack of sectioning may facilitate faster imaging speeds in some applications by aggregating fluorescence signals acquired simultaneously from adjacent tissue depths. The key advantage of two-photon imaging is robustness to scattering and increased penetration depths, but the high cost of an ultrashort-pulse laser is a distinct disadvantage. Nonetheless, when using epifluorescence or confocal modalities to image through more than ~50 μm of tissue, image contrast declines sharply with depth due to scattering. Additionally, these two modalities are more vulnerable to photobleaching and phototoxicity, which unlike in two-photon imaging occur not only at the focus but also in out-of-focus planes.

Epifluorescence imaging modalities

One-photon epifluorescence imaging can involve a compound GRIN microendoscope probe, a flexible fiber bundle or both. Unlike existing forms of either fiber-optic confocal or two-photon imaging, one-photon endoscopy and microendoscopy are currently the only fiber imaging varieties that enable images to be directly viewed by eye.

In the simplest form of one-photon FME (Fig. 4a), a conventional microscope is equipped with a GRIN endoscope probe ≤1 mm in diameter. The microscope objective directs illumination light into the probe and adjustment of the objective position provides a noninvasive focusing mechanism for altering the image plane in the tissue[35,36].

Figure 3 | An MEMS scanner. (**a**) Scanning electron micrograph of 2D MEMS vertical comb scanner. Electrostatically driven angular vertical comb actuators rotate the 1-mm-diameter mirror about the torsion beams. Gimbal mounting of the mirror and actuators allows 2D scanning. Scale bar, 500 μm. (**b**) Scanning electron micrograph of vertical comb actuators. Scale bar, 100 μm. Material is this figure is based on work by Piyawattanametha *et al.*[71]

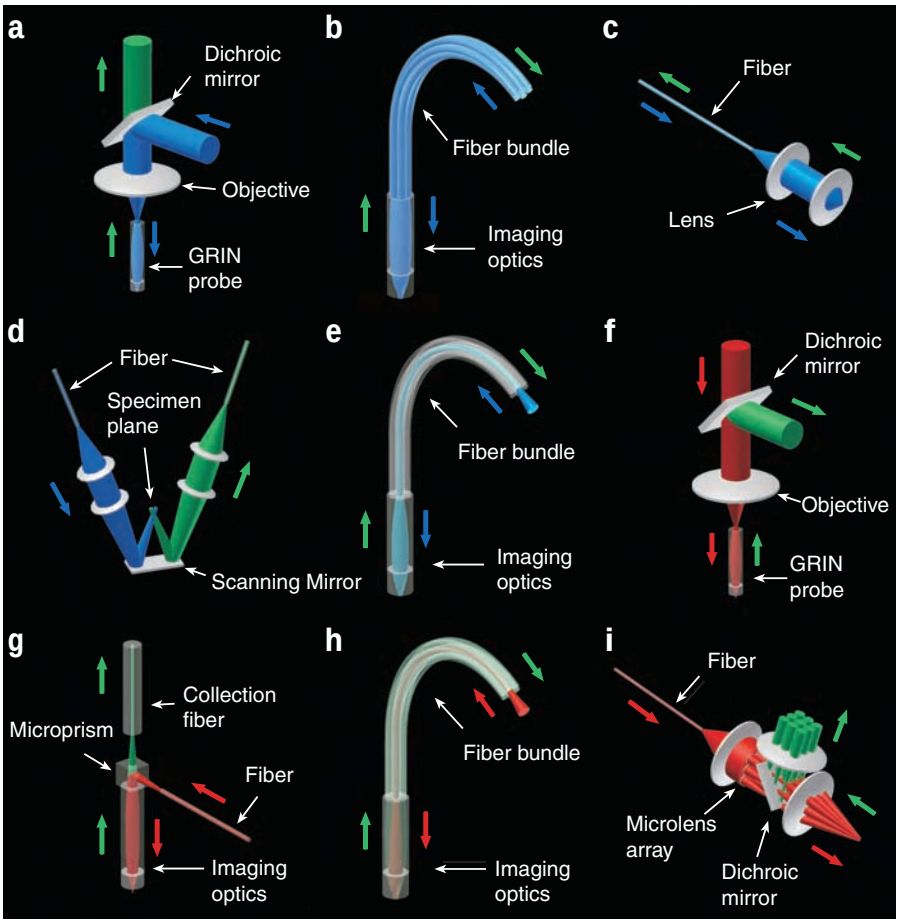

Figure 4 | Fiber-optic fluorescence imaging embodiments. (**a**) One-photon FME using a GRIN microendoscope probe. Visible illumination is coupled into the probe, which focuses the light onto the sample. Fluorescence returns through the probe. (**b**) One-photon epifluorescence imaging using a fiber bundle. Illumination travels through the fiber bundle to a small objective or GRIN lens, which focuses the light onto the sample. Fluorescence returns through the bundle. (**c**) Confocal imaging using SMF. The SMF delivers illumination to lenses that collimate and focus the light onto the specimen. The SMF core also serves as a pinhole for collecting in focus but rejecting out-of-focus fluorescence emissions. For microscopy, this embodiment generally relies on galvanometer scanning mirrors, which would be located between the fiber and lenses. For flexible endoscopy, the miniaturized distal scanning mechanisms are appropriate. (**d**) Dual-axis confocal microscopy. One SMF delivers excitation light and a second SMF, mounted at an angle with respect to the first, collects fluorescence from the overlapping region of the two fiber apertures. (**e**) Fiber bundle confocal imaging. Visible excitation light is scanned across a fiber bundle. A miniaturized objective or GRIN lens focuses the light onto the sample. Fluorescence returns through the probe and is routed to a pinhole detector. (**f**) Two-photon FME with a GRIN microendoscope probe. Ultrashort pulses are coupled into the probe, which focuses the light onto the sample. Fluorescence returns back through the probe and is routed to a photodetector. (**g**) Single-fiber two-photon imaging. Ultrashort pulses exiting a single fiber are scanned in 2D before entering a miniaturized objective or GRIN lens, which focuses the near-infrared excitation pulses onto the sample. A coated microprism can serve as a dichroic mirror. A large-core multimode fiber collects fluorescence. (**h**) Fiber bundle two-photon imaging. Ultrashort pulses are scanned across the proximal end of a fiber bundle. A miniature objective or GRIN lens focuses the light onto the sample. Fluorescence returns through the bundle to a detector. (**i**) Multifocal two-photon imaging. A single fiber delivers the excitation light to a collimating lens. A micro-lens array divides the beam into multiple 'beamlets', which are scanned in 2D and focused onto the sample. In all panels, blue represents visible fluorescence excitation light, red represents ultrashort-pulsed near-infrared light for two-photon excitation, and green represents visible fluorescence emission. Arrows show the directions of light propagation. Detectors and cameras are omitted. Scanners and dichroic mirrors are not shown except where explicitly labeled.

This approach has enabled imaging of neuronal activity and blood flow in deep brain regions of live rodents[2,35,79], but the use of short, rigid microendoscope probes coupled to a full-sized microscope restricts applications to immobilized specimens.

The use of fiber bundles alleviates this stipulation and provides mechanical flexibility while imaging in deep tissue[59] (Fig. 4b). Similar approaches have been used for reflectance imaging in freely moving cats[80]. With a bare fiber bundle, only objects in direct contact with the tip of the bundle are in focus, but addition of a miniature lens to the distal end of the bundle can add optical working distance. As with conventional epifluorescence microscopy, out-of-focus and scattered fluorescence photons reduce image contrast.

Confocal imaging modalities

Fiber-optic confocal imaging can involve one SMF, two SMFs for dual-axis imaging or a fiber bundle. SMFs are used in confocal microscopy for remote light delivery, but their main application is in flexible endoscopy. Miniaturized optics and compact distal scanning mechanisms, such as fiber-tip scanning[22,65] (Fig. 2e), fiber-objective lens scanning[20,24,67] (Fig. 2f) or MEMS mirror–based scanning (Figs. 2d and 3)[68,69], have enabled SMF-based confocal endoscopes with an outer diameter as small as 3.5 mm (Fig. 4c)[24]. Nonetheless, reduction of imaging and scanning optics to the millimeter scale nearly always compromises some combination of resolution, field of view and working distance. With confocal endoscopy based on one SMF (Fig. 4c), design pressures tend to center on the choice of high NA objective optics, which are a key determinant of image quality and fluorescence collection efficiency.

Dual-axis confocal imaging provides an alternate set of compromises, reducing ease of alignment and efficiency of fluorescence collection to gain longer optical working distance, immunity to off-axis aberrations, and good axial resolution using economical objective lenses. Two SMFs mounted at an angle to one another deliver light and collect fluorescence, respectively (Fig. 4d). Axial resolution is determined by the angle between the fibers and the transverse size of the illumination beam. Thus, two low-NA, long-working-distance objectives can provide an effective high-NA for axial sectioning, although the fluorescence collection NA remains low. A compact postobjective scanning

mechanism, such as a 2D tip-tilt mirror (Fig. 2d), offers broad fields of view up to ~500 μm[81–83]. To date, dual-axis imaging has been demonstrated in microscopy, but dual-axis endoscopy should emerge soon.

Fiber bundle confocal imaging facilitates miniaturization by use of conventional scanners proximal to the light source but reduces resolution through image pixilation (Fig. 4e). Many fiber bundle confocal designs also forgo a focusing mechanism to reduce size. For example, simply fusing a compound GRIN micro-lens onto the tip of a bundle enables handheld confocal FME probes with diameters as small as 300 μm[40,42]. Such probes and accompanying imaging systems are now commercially available. By comparison, fiber bundle confocal endoscopes with remotely controlled distal focusing and miniature objective lenses exist with outer diameters as small as 3 mm[30]. With either variety, a descanning pinhole rejects out-of-focus fluorescence to achieve optical sectioning. Scanning a line of excitation light across the bundle (Fig. 2b) boosts the image-acquisition rate, enabling video-rate imaging, although one must then use a descanning slit that does not reject out-of-focus light along the slit's linear dimension[25,30,31].

Two-photon fluorescence imaging modalities

For two-photon FME, a conventional two-photon microscope can be furnished with a GRIN microendoscope probe for insertion into tissue (Fig. 4f). As in one-photon FME, adjustment of the microscope objective position alters image focus. Although image frame rates have been lower (up to several Hz) than in one-photon FME, localized two-photon excitation provides inherent optical sectioning up to hundreds of micrometers from the tip of the endoscope probe. Two-photon FME has enabled *in vivo* imaging of individual neurons and blood vessels deep in the brain[35,37].

As with one-photon endoscopy, the combination of a short endoscope probe and a flexible fiber removes the requirement for specimens to be immobilized (Fig. 4g). A two-photon FME system based on a PBF for delivery of ultrashort pulses and a GRIN microendoscope probe has been created with an imaging head that is ~3.5 cm × 1.2 cm × 1.5 cm in size and 3.9 g in mass[38]. This device uses resonant fiber tip scanning[1], DC micromotor–based focusing and collection of fluorescence using a large-core multimode fiber. By comparison, fiber-optic two-photon microscopy based on a small microscope objective provides finer resolution and higher collection efficiency but does not allow the same degree of miniaturization[1].

For both flexibility and superior miniaturization, a fiber bundle based approach to two-photon FME has been realized (Fig. 4h)[39]. Because fluorescence excitation is localized to the focal spot, the descanning pinhole of confocal modalities is unnecessary, enabling whole-area detection in which fluorescence is collected across the entire bundle. Nonlinear distortion of the excitation pulses in each fiber (Box 1) currently limits fiber-bundle two-photon imaging to applications in surface tissue that do not require nanojoule energy pulses[39]. Unfortunately, arrays of hollow core PBF or LMA-PCF do not yet exist with sufficiently large numbers of pixels for imaging.

The combination of a single PBF for light delivery, a micro-lens array for generating multiple foci and a small 2D scanning mirror has enabled high-speed, handheld two-photon microscopy (Fig. 4i)[17,18]. Because multiple laser foci exist within the sample it is necessary to use a camera or multianode photomultiplier tube for signal detection. When the field of view is small and imaging is performed deep within tissue, scattering of fluorescence emissions can lead to cross talk between pixels and reduced contrast. To date, multifocal, two-photon imaging has been demonstrated for portable microscopy[17,18], but further miniaturization might enable endoscopy.

FUTURE DIRECTIONS

Fiber-optic fluorescence imaging will continue to benefit from progress in miniaturized and microfabricated components. There is also growing interest in other nonlinear optical modalities, such as second harmonic generation (SHG)[84] and Coherent Anti-Stokes Raman Scattering (CARS)[85], that provide inherent optical sectioning as in two-photon imaging but with intrinsic contrast generation mechanisms that do not require a dye label. Fiber-optic SHG and CARS imaging will benefit from the same trends towards miniaturization that are driving progress in fiber-optic fluorescence imaging.

Future fiber-optic systems will likely use microfabricated components in addition to scanning mirrors. Electrostatically actuated lenses are an alternative to MEMS mirrors for miniaturized scanning[86]. In addition, optical fibers and small lenses can be integrated by micromachining a v-groove or optical benches directly into a silicon wafer[68,87,88]. Optical fibers for light delivery and collection may eventually become unnecessary with the advent of integrated semiconductor laser sources and photodetectors[89]. Imaging systems in which all components are fabricated monolithically would provide a new degree of miniaturization, inherent alignment and potential for highly parallel imaging. Together, such advances will propel imaging applications that require both portability and a high degree of functionality.

ACKNOWLEDGMENTS

Our work on fiber-optic imaging is supported by grants to M.J.S from the Human Frontier Science Program, the US National Institute on Drug Abuse, the US National Institute of Neurological Disorders and Stroke, the US National Science Foundation, the US Office of Naval Research, the Arnold & Mabel Beckman Foundation and the David & Lucille Packard Foundation. B.A.F is a National Science Foundation Graduate Research Fellow. E.D.C. is a member of the Stanford Biotechnology Program. W.P. is an affiliate of the National Electronics and Computer Technology Center of Thailand. E.L.M.C. is supported in part by a Dean's Fellowship, Stanford School of Medicine. We thank R. Kristiansen of C. Fibre for providing images of photonic crystal fiber.

COMPETING INTERESTS STATEMENT

The authors declare that they have no competing financial interests.

Published online at http://www.nature.com/naturemethods/
Reprints and permissions information is available online at http://npg.nature.com/reprintsandpermissions/

1. Helmchen, F., Fee, M.S., Tank, D.W. & Denk, W. A miniature head-mounted two-photon microscope. high-resolution brain imaging in freely moving animals. *Neuron* **31**, 903–912 (2001).
2. Monfared, A. *et al. In vivo* imaging of mammalian cochlear blood flow using fluorescence microendoscopy. *Otol. Neurotol.* (in the press) .
3. Bashford, C.L., Barlow, C.H., Chance, B., Haselgrove, J. & Sorge, J. Optical measurements of oxygen delivery and consumption in gerbil cerebral cortex. *Am. J. Physiol.* **242**, C265–C271 (1982).
4. Chance, B., Cohen, P., Jobsis, F. & Schoener, B. Intracellular oxidation-reduction states *in vivo*. *Science* **137**, 499–508 (1962).
5. Mayevsky, A. & Chance, B. Intracellular oxidation-reduction state measured *in situ* by a multichannel fiber-optic surface fluorometer. *Science* **217**, 537–540 (1982).
6. Epstein, J.R. & Walt, D.R. Fluorescence-based fibre optic arrays: a universal platform for sensing. *Chem. Soc. Rev.* **32**, 203–214 (2003).
7. Yamaguchi, S. *et al.* View of a mouse clock gene ticking. *Nature* **409**, 684 (2001).
8. Bird, D. & Gu, M. Fibre-optic two-photon scanning fluorescence microscopy. *J. Microsc.* **208**, 35–48 (2002).
9. Ghiggino, K.P., Harris, M.R. & Spizzirri, P.G. Fluorescence lifetime measurements using a novel fiber-optic laser scanning confocal microscope. *Rev. Sci. Instrum.*

63, 2999–3002 (1992).
10. Dabbs, T. & Glass, M. Fiber optic confocal microscope: FOCON. *Appl. Opt.* **31**, 3030–3035 (1992).
11. Bird, D. & Gu, M. Compact two-photon fluorescence microscope based on a single-mode fiber coupler. *Opt. Lett.* **27**, 1031–1033 (2002).
12. Bird, D. & Gu, M. Resolution improvement in two-photon fluorescence microscopy with a single-mode fiber. *Appl. Opt.* **41**, 1852–1857 (2002).
13. Delaney, P.M., Harris, M.R. & King, R.G. Novel microscopy using fibre optic confocal imaging and its suitability for subsurface blood vessel imaging *in vivo*. *Clin. Exp. Pharmacol. Physiol.* **20**, 197–198 (1993).
14. Delaney, P.M., Harris, M.R. & King, R.G. Fiber-optic laser scanning confocal microscope suitable for fluorescence imaging. *Appl. Opt.* **33**, 573–577 (1994).
15. Delaney, P.M., King, R.G., Lambert, J.R. & Harris, M.R. Fibre optic confocal imaging (FOCI) for subsurface microscopy of the colon *in vivo*. *J. Anat.* **184**, 157–160 (1994).
16. Tai, S.P. *et al.* Two-photon fluorescence microscope with a hollow-core photonic crystal fiber. *Opt. Express* **12**, 6122–6128 (2004).
17. Kim, D., Kim, K.H., Yazdanfar, S. & So, P.T.C. Optical biopsy in high-speed handheld miniaturized multifocal multiphoton microscopy. *Proceedings of SPIE* **5700**, 14–22 (2005).
18. Kim, D., Kim, K.H., Yazdanfar, S. & So, P.T.C. High speed handheld multiphoton multifoci microscopy. *Proceedings of SPIE* **5323**, 267–272 (2004).
19. Carlson, K. *et al. In vivo* fiber-optic confocal reflectance microscope with an injection-molded miniature objective lens. *Appl. Opt.* **44**, 1792–1796 (2005).
20. Giniunas, L., Juskaitis, R. & Shatalin, S.V. Scanning fibre-optic microscope. *Electronics Lett.* **27**, 724–726 (1991).
21. Giniunas, L., Juskaitis, R. & Shatalin, S.V. Endoscope with optical sectioning capability. *Appl. Opt.* **32**, 2888–2890 (1993).
22. Kiesslich, R. *et al.* Confocal laser endoscopy for diagnosing intraepithelial neoplasias and colorectal cancer *in vivo*. *Gastroenterology* **127**, 706–713 (2004).
23. Liang, C., Sung, K.B., Richards-Kortum, R. & Descour, M.R. Design of a high-numerical aperture miniature microscope objective for an endoscopic fiber confocal reflectance microscope. *Appl. Opt.* **41**, 4603–4610 (2002).
24. Ota, T., Fukuyama, H., Ishihara, Y., Tanaka, H. & Takamatsu, T. *In situ* fluorescence imaging of organs through compact scanning head for confocal laser microscopy. *J. Biomed. Opt.* **10**, 1–4 (2005).
25. Rouse, A.R. & Gmitro, A.F. Multispectral imaging with a confocal microendoscope. *Opt. Lett.* **25**, 1708–1710 (2000).
26. Swindle, L.D., Thomas, S.G., Freeman, M. & Delaney, P.M. View of normal human skin *in vivo* as observed using fluorescent fiber-optic confocal microscopic imaging. *J. Invest. Dermatol.* **121**, 706–712 (2003).
27. Anikijenko, P. *et al. In vivo* detection of small subsurface melanomas in athymic mice using noninvasive fiber optic confocal imaging. *J. Invest. Dermatol.* **117**, 1442–1448 (2001).
28. Bussau, L.J. *et al.* Fibre optic confocal imaging (FOCI) of keratinocytes, blood vessels and nerves in hairless mouse skin *in vivo*. *J. Anat.* **192**, 187–194 (1998).
29. Papworth, G.D., Delaney, P.M., Bussau, L.J., Vo, L.T. & King, R.G. *In vivo* fibre optic confocal imaging of microvasculature and nerves in the rat vas deferens and colon. *J. Anat.* **192**, 489–495 (1998).
30. Rouse, A.R., Kano, A., Udovich, J.A., Kroto, S.M. & Gmitro, A.F. Design and demonstration of a miniature catheter for a confocal microendoscope. *Appl. Opt.* **43**, 5763–5771 (2004).
31. Sabharwal, Y.S., Rouse, A.R., Donaldson, K.A., Hopkins, M.F. & Gmitro, A.F. Slit-scanning confocal microendoscope for high-resolution *in vivo* imaging. *Appl. Opt.* **38**, 7133–7144 (1999).
32. McLaren, W., Anikijenko, P., Barkla, D., Delaney, T.P. & King, R. *In vivo* detection of experimental ulcerative colitis in rats using fiberoptic confocal imaging (FOCI). *Dig. Dis. Sci.* **46**, 2263–2276 (2001).
33. McLaren, W.J., Anikijenko, P., Thomas, S.G., Delaney, P.M. & King, R.G. *In vivo* detection of morphological and microvascular changes of the colon in association with colitis using fiberoptic confocal imaging (FOCI). *Dig. Dis. Sci.* **47**, 2424–2433 (2002).
34. Vo, L.T. *et al.* Autofluorescence of skin burns detected by fiber-optic confocal imaging: evidence that cool water treatment limits progressive thermal damage in anesthetized hairless mice. *J. Trauma* **51**, 98–104 (2001).
35. Jung, J.C., Mehta, A.D., Aksay, E., Stepnoski, R. & Schnitzer, M.J. *In vivo* mammalian brain imaging using one- and two-photon fluorescence microendoscopy. *J. Neurophysiol.* **92**, 3121–3133 (2004).
36. Jung, J.C. & Schnitzer, M.J. Multiphoton endoscopy. *Opt. Lett.* **28**, 902–904 (2003).
37. Levene, M.J., Dombeck, D.A., Kasischke, K.A., Molloy, R.P. & Webb, W.W. *In vivo* multiphoton microscopy of deep brain tissue. *J. Neurophysiol.* **91**, 1908–1912 (2004).
38. Flusberg, B.A., Jung, J.C., Cocker, E.D., Anderson, E.P. & Schnitzer, M.J. *In vivo* brain imaging using a portable 3.9 gram two-photon fluorescence microendoscope. *Opt. Lett.* **30**, 2272–2274 (2005).
39. Gobel, W., Kerr, J.N., Nimmerjahn, A. & Helmchen, F. Miniaturized two-photon microscope based on a flexible coherent fiber bundle and a gradient-index lens objective. *Opt. Lett.* **29**, 2521–2523 (2004).
40. Knittel, J., Schnieder, L., Buess, G., Messerschmidt, B. & Possner, T. Endoscope-compatible confocal microscope using a gradient index-lens system. *Opt. Commun.* **188**, 267–273 (2001).
41. D'Hallewin, M-A., Khatib, S.E., Leroux, A., Bezdetnaya, L. & Guillemin, F. Endoscopic confocal fluorescence microscopy of normal and tumor bearing rat bladder. *J. Urol.* **174**, 736–740 (2005).
42. Laemmel, E. *et al.* Fibered confocal fluorescence microscopy (Cell-viZio™) facilitates extended imaging in the field of microcirculation. A comparison with intravital microscopy. *J. Vasc. Res.* **41**, 400–411 (2004).
43. Bird, D. & Gu, M. Two-photon fluorescence endoscopy with a micro-optic scanning head. *Opt. Lett.* **28**, 1552–1554 (2003).
44. Mehta, A.D., Jung, J.C., Flusberg, B.A. & Schnitzer, M.J. Fiber optic *in vivo* imaging in the mammalian nervous system. *Curr. Opin. Neurobiol.* **14**, 617–628 (2004).
45. Saleh, B.E.A. & Teich, M.C. *Fundamentals of photonics* (John Wiley & Sons, Inc., New York, USA, 1991).
46. Harris, M.R. (US patent 5120953, 1992).
47. Fu, L., Gan, X. & Gu, M. use of a single-mode fiber coupler for second-harmonic-generation microscopy. *Opt. Lett.* **30**, 385–387 (2005).
48. Yariv, A. Three-dimensional pictorial transmission in optical fibers. *Appl. Phys. Lett.* **28**, 88–89 (1976).
49. Helmchen, F., Tank, D.W. & Denk, W. Enhanced two-photon excitation through optical fiber by single-mode propagation in a large core. *Appl. Opt.* **41**, 2930–2934 (2002).
50. Myaing, M.T., Urayama, J., Braun, A. & Norris, T.B. Nonlinear propagation of negatively chirped pulses: Maximizing the peak intensity at the output of a fiber probe. *Opt. Express* **7**, 210–214 (2000).
51. Ouzounov, D.G. *et al.* Delivery of nanojoule femtosecond pulses through large-core microstructured fibers. *Opt. Lett.* **27**, 1513–1515 (2002).
52. Knight, J.C. Photonic crystal fibres. *Nature* **424**, 847–851 (2003).
53. Gobel, W., Nimmerjahn, A. & Helmchen, F. Distortion-free delivery of nanojoule femtosecond pulses from a Ti:sapphire laser through a hollow-core photonic crystal fiber. *Opt. Lett.* **29**, 1285–1287 (2004).
54. Tai, S.-H., Chan, M.-C., Tsai, T.-H., Guol, S.-H., Chen, L.-J. & Sun, C.-K. Two-photon fluorescence microscope with a hollow-core photonic crystal fiber. *Proceedings of SPIE* **5691**, 146–152 (2005).
55. Treacy, E.B. Optical pulse compression with diffraction gratings. *IEEE J. Quantum Electron.* **QE-5**, 454–458 (1969).
56. Fork, R.L., Brito Cruz, C.H., Becker, P.C. & Shank, C.V. Compression of optical pulses to six femtoseconds by using cubic phase compensation. *Opt. Lett.* **12**, 483–485 (1987).
57. Ye, J.Y. *et al*. Development of a double-clad photonic-crystal-fiber based scanning microscope. *Proceedings of SPIE* **5700**, 23–27 (2005).
58. Fu, L., Gan, X. & Gu, M. Nonlinear optical microscopy based on double-clad photonic crystal fibers. *Opt. Express* **13**, 5528–5534 (2005).
59. Hirano, M., Yamashita, Y. & Miyakawa, A. *In vivo* visualization of hippocampal cells and dynamics of Ca2+ concentration during anoxia: feasibility of a fiber-optic plate microscope system for *in vivo* experiments. *Brain Res.* **732**, 61–68 (1996).
60. Lane, P.M., Dlugan, A.L.P., Richards-Kortum, R. & MacAulay, C.E. Fiber-optic confocal microscopy using a spatial light modulator. *Opt. Lett.* **25**, 1780–1782 (2000).
61. Gmitro, A.F. & Aziz, D. Confocal microscopy through a fiber-optic imaging bundle. *Opt. Lett.* **18**, 565–567 (1993).
62. Lin, C.H. & Webb, R.H. Fiber-coupled multiplexed confocal microscope. *Opt. Lett.* **25**, 954–957 (2000).
63. Dong, C.Y., Koenig, K. & So P. Characterizing point spread functions of two-photon fluorescence microscopy in turbid medium *J. Biomed. Opt.* **8**, 450–459 (2003).
64. Seibel, E.J. & Smithwick, Q.Y. Unique features of optical scanning, single fiber endoscopy. *Lasers Surg. Med.* **30**, 177–183 (2002).
65. Delaney, P.M. & Harris, M.R. In *Handbook of Biological Confocal Microscopy* (ed. Pawley, J. B.) 515–523 (Plenum Press, New York, 1995).
66. Harris, M.R. (UK patent W09904301, 1999).
67. Dickensheets, D. & Kino, G.S. Scanned optical fiber confocal microscope. *Proceedings of SPIE* **2184**, 39–47 (1994).
68. Dickensheets, D.L. & Kino, G.S. Micromachined scanning confocal optical microscope. *Opt. Lett.* **21**, 764–766 (1996).
69. Hofmann, U., Muehlmann, S., Witt, M., Dorschel, K., Schutz, R. & Wagner, B. Electrostatically driven micromirrors for a miniaturized confocal laser scanning microscope. *Proceedings of SPIE* **3878**, 29–38 (1999).
70. Piyawattanametha, W., Toshiyoshi, H., LaCosse, J. & Wu, M.C. Surface

micromachined confocal scanning optical microscope. In *Technical Digest Series of Conference on Lasers and Electro-Optics (CLEO),* 447–448 (San Francisco, 2000).
71. Piyawattanametha, W., Patterson, P., Hah, D., Toshiyoshi, H. & Wu, M.C. A 2D scanner by surface and bulk micromachined angular vertical comb actuators. In *IEEE/LEOS International Conference on Optical MEMS,* 93–94 (Waikoloa, Hawaii, 2003).
72. Schenk, H. *et al.* Large deflection micromechanical scanning mirrors for linear scans and pattern generation. *J. Select. Topics in Quantum Electronics* **6**, 715–722 (2000).
73. Lee, D. Solgaard, O. T. Two-axis gimbaled microscanner in double SOI layers actuated by self-aligned vertical electrostatic combdrive. In *Proceedings of the Solid-State Sensor and Actuator Workshop,* 352–355 (Hilton Head, South Carolina, 2004).
74. Rector, D.M., Rogers, R.F. & George, J.S. A focusing image probe for assessing neural activity *in vivo*. *J. Neurosci. Methods* **91**, 135–145 (1999).
75. Kuiper, S. & Hendriks, B.H.W. Variable-focus liquid lens for miniature cameras. *Appl. Phys. Lett.* **85**, 1128–1130 (2004).
76. Berge, B. & Peseux, J. Variable focal lens controlled by an external voltage: an application of electrowetting. *Eur. Phys. J. E* **3**, 159–163 (2000).
77. Kuiper, S., Hendriks, B.H.W., Hayes, R.A., Feenstra, B.J. & Baken, J.M.E. Electrowetting-based optics. *Proceedings of SPIE* **5908**, 5908OR-1–5908OR-7 (2005).
78. George, M. Optical methods and sensors for *in situ* histology in surgery and endoscopy. *Min. Invas. Ther. & Allied. Technol.* **13**, 95–104 (2004).
79. Fisher, J.A.N., Civillico, E.F., Contreras, D. & Yodh, A.G. *In vivo* fluorescence microscopy of neuronal activity in three dimensions by use of voltage-sensitive dyes. *Opt. Lett.* **29**, 71–73 (2004).
80. Poe, G.R., Rector, D.M. & Harper, R.M. Hippocampal reflected optical patterns during sleep and waking states in the freely behaving cat. *J. Neurosci.* **14**, 2933–2942 (1994).
81. Wang, T.D., Contag, C.H., Mandella, M.J., Chan, N.Y. & Kino, G.S. Dual-axes confocal microscopy with post-objective scanning and low-coherence heterodyne detection. *Opt. Lett.* **28**, 1915–1917 (2003).
82. Wang, T.D., Contag, C.H., Mandella, M.J., Chan, N.Y. & Kino, G.S. Confocal fluorescence microscope with dual-axis architecture and biaxial postobjective scanning. *J. Biomed. Opt.* **9**, 735–742 (2004).
83. Wang, T.D., Mandella, M.J., Contag, C.H. & Kino, G.S. Dual-axis confocal microscope for high resolution *in vivo* imaging. *Opt. Lett.* **28**, 414–416 (2003).
84. Brown, E. *et al.* Dynamic imaging of collagen and its modulation in tumors *in vivo* using second-harmonic generation. *Nat. Med.* **9**, 796–800 (2003).
85. Cheng, J.-X., & Xie, X.S. Coherent anti-Stokes Raman scattering microscopy: instrumentation theory, and applications. J. Phys. Chem. B 108, 827–840 (2004).
86. Kwon, S. & Lee, L.P. Micromachined transmissive scanning confocal microscope. *Opt. Lett.* **29**, 706–708 (2004).
87. Lee, K.-N., Jang, Y.-H., Choi, J. & Kim, H. Silicon scanning mirror with 54.74° slanted reflective surface for fluorescence scanning system. *Proceedings of SPIE* **5641**, 56–66 (2004).
88. Sheard, S., Suhara, T. & Nishihara, H. Integrated-optic implementation of a confocal scanning optical microscope. *Journal of Lightwave Technology* **11**, 1400–1403 (1993).
89. Thrush, E. *et al.* Integrated semiconductor verticle-cavity surface-emitting lasers and PIN photodetectors for biomedical fluorescence sensing. *IEEE J. Quantum Electron.* **40**, 491–498 (2004).
90. McConnell, G. & Riis, E. Photonic crystal fibre enables short-wavelength two-photon laser scanning fluorescence microscopy with fura-2. *Phys. Med. Biol.* **49**, 4757–4763 (2004).
91. McConnell, G. & Riis, E. Two-photon laser scanning fluorescence microscopy using photonic crystal fiber. *J. Biomed. Opt.* **9**, 922–927 (2004).